Bull. Mater. Sci. (2020) 43:18
https://doi.org/10.1007/s12034-019-1967-1

Antibacterial activity of ZnO nanoflowers deposited on biodegradable acrylic acid hydrogel by chemical bath deposition

SINAN TEMEL, FATMA OZGE GOKMEN* and ELIF YAMAN
Central Research Laboratory, Bilecik Şeyh Edebali University, 11230 Bilecik, Turkey
*Author for correspondence (fatmaozge.gokmen@bilecik.edu.tr)

MS received 23 October 2018; accepted 12 June 2019; published online 18 December 2019

Abstract. In the first part of this study, acrylic acid (AA) hydrogels were produced by a free radical reaction. Chemical and morphological structures of AA-hydrogels were specified by using Fourier transform infrared (FT-IR) spectroscopy and scanning electron microscopy (SEM) techniques. In the second part of the study, ZnO nanoflowers were synthesized on the AA-hydrogel by using a chemical bath deposition (CBD) technique for the first time in the literature. The AA-hydrogel acted as the substrate in the CBD process. The deposition time effect on the morphological properties of ZnO nanoflowers was determined by applying SEM. According to the SEM results, the deposition time in the production of ZnO nanoflowers has played a vital role in the surface morphology. Chemical, morphological and thermal properties of the ZnO nanoflowers were determined by applying FT-IR, scanning electron microscopy-energy dispersive X-ray spectroscopy and thermogravimetric analysis techniques. Elemental mapping of ZnO nanostructures was carried out using SEM. The antibacterial activity of the ZnO nanoflower-deposited AA-hydrogel was determined against Gram-negative and Gram-positive bacteria. *Escherichia coli* (*E. coli*) and *Staphylococcus aureus* (*S. aureus*) were used as test microorganisms. Gram-negative bacteria were more resistant to hydrogels and ZnO nanoflowers compared to Gram-positive bacteria.

Keywords. AA-hydrogel; chemical bath deposition; nanomaterials; ZnO; antibacterial activity.

1. Introduction

Nanoparticles are the most important group of materials with extensive application [1]. These materials have unique properties in comparison with their bulk size counterparts [2,3]. These unique properties provide an opportunity for the development of nanoparticles for use as antibacterial agents.

In recent years, there has been an increasing interest about inorganic compounds in nano-size. Due to their high-surface area and unique chemical and physical properties, inorganic compounds in nano-size show strong antibacterial properties even if they used low concentrations [4]. The higher surface area of nano-sized particles provides probable interactions with biologic systems existing on the viable cell surface [5]. The other advantage of nano-sized particles is being more stable at high temperature and pressure conditions [6]. Some of the nano-particles are nontoxic and they can involve mineral elements essential to the human body [7]. ZnO, MgO, TiO_2 and SiO_2 show substantial antibacterial properties and their selective toxicity to biological systems provides their potential application as therapeutics, diagnostics, surgical devices and nanomedicine-based antimicrobial agents [6,8–11].

Hydrogels are also another important material in these applications with their biocompatibility properties. Hydrogels are three-dimensional materials which have critical crosslink provided by covalent bonds, hydrogen bondings and van der Waals interactions. An increasing interest on hydrogels as antibacterial materials or substrates is due to their superior biomedical relevance [12]. Through the biocompatible hydrogels, the metal oxide-doped nanocomposite hydrogels are particularly promising to decrease bacterial growth.

ZnO nano-particles are one of the most important multifunctional inorganic nanoparticles with their chemical and physical stabilities, high-catalysis activity, effective antibacterial activity as well as intensive ultraviolet and infrared adsorption with a broad range of applications as semiconductors, sensors, transparent electrodes, solar cells, etc. [1,13]. The ZnO nanoflower doped on the biodegradable hydrogel is an alternative way to widely use over-priced nano-particles such as silver. However, there are only a few studies about ZnO nanoflowers on biodegradable hydrogels [12].

In this study, the ZnO nanoflower was deposited on an acrylic acid (AA) hydrogel by a chemical bath deposition (CBD) technique. ZnO nano-particles can be produced *via* Amiri followed by Nosaka [3], biosynthesis [14,15], solvothermal [16] or sol–gel [17] methods. Among these various techniques of the production of ZnO nano-particles, the CBD technique is a vacuum-free, safe, environmentally friendly, economic and easy technique. In the literature, there is no study about the production of nanoflowers like ZnO on the hydrogel substrate. The novelty of the study is the characterization and specification of antibacterial properties of ZnO nanoflowers on the hydrogel *via* CBD.

2. Experimental

The biodegradable hydrogel and ZnO nanoflowers synthesized as well as the techniques that were used for their preparation and the characterization of their properties are described in this section.

2.1 *Preparation of the AA biodegradable hydrogel*

The cross-linked biodegradable hydrogels were prepared *via* an *in situ* free radical reaction. AA, N,N'-methylene-bis-acrylamide and ammonium per sulphate were used as the monomer, cross-linking agent and initiator, respectively. Experimental details were given in the previous study [18].

2.2 *Deposition of the ZnO nanoflower on the AA biodegradable hydrogel*

The ZnO nanoflower was deposited on an AA biodegradable hydrogel by the CBD technique. Zinc nitrate hexahydrate $Zn(NO_3)_2{\cdot}6H_2O$ (Sigma Aldrich) was used as the zinc source. pH was fixed to 10 with adding ammonia solution (28% v/v) (Merck) drop by drop. To observe the time effect on the ZnO nanoflower structure, the bath solution was stirred using a temperature-controlled magnetic stirrer at 85°C for 15, 30, 45 and 60 min. Experimental details were given in previous studies [19,20].

2.3 *Characterization techniques*

Thermal stabilities of the produced AA biodegradable hydrogel and ZnO nanoflower-deposited hydrogel were determined by using a thermogravimetric analyser (Seteram, LabSys-Evo). A sample mass of 10 ± 3 mg in the Al_2O_3 crucible was used for each run. The samples were heated from 25 to 900°C with a heating rate of 10°C min^{-1}. Nitrogen (20 ml min^{-1}) was used as the carrier gas.

Fourier-transform infrared (FT-IR) analysis (Perkin Elmer, Spectrum 100) was performed to indicate various surface functional groups of samples in the transmission mode between 4000 and 400 cm^{-1}.

To specify the morphologies of the samples, a sputter coater (Quorum-Q150R) was used to provide sample conductivity. Images were recorded using a Supra 40VP scanning electron microscopy (SEM) operating at 15 kV using a secondary electron detector. Zinc and oxygen distributions in the AA biodegradable hydrogel were identified by applying the mapping method (Bruker EDX detector).

2.4 *Test of antibacterial activity*

The antibacterial activity tests were carried out in accordance with ASTME2149 (determining the antimicrobial activity of antimicrobial agents under dynamic contact conditions) with the bacteria *Staphylococcus aureus* ATCC 6538 and *Escherichia coli* ATCC 8739.

3. Results and discussion

In this section, the results from the characterization of the hydrogel as well as the ZnO nanoflower on the hydrogel are presented and discussed.

3.1 *Characterization of the ZnO nanoflower on the AA biodegradable hydrogel in various deposition times*

The morphology of the ZnO nanoflower on the AA biodegradable hydrogel was determined by SEM images. Figure 1 represents the SEM micrographs of the ZnO nanoflower synthesized at different deposition times. The high-resolution SEM images show ZnO nanoflowers at 15 min that are not fully developed. Further SEM images at 30 min show fully developed nanoflowers with narrow particle-size distribution. It is also seen that the samples synthesized at 45 and 60 min are broken down and dispersed in a disordered manner on the AA hydrogel surface. According to the SEM results, it was decided to compare the AA biodegradable hydrogel and ZnO nanoflowers on the AA biodegradable hydrogel which was synthesized at 30 min.

Elemental analysis and mapping results of the ZnO nanoflower on the AA biodegradable hydrogel are shown in figure 2. Figure 2a shows the mapping scanning area and figure 2b shows the elemental content of the sample. The ZnO nanoflower on the AA biodegradable hydrogel contains carbon, oxygen and zinc with an atomic percentage of 39.36, 45.45 and 15.19%, respectively. Figure 2c and d proves that zinc and oxygen disperse on the hydrogel surface homogeneously.

3.2 *Characterization of the AA biodegradable hydrogel and ZnO nanoflower on the AA biodegradable hydrogel*

FT-IR spectroscopy was used to determine the presence or absence of the various vibrational modes present in the samples. The FT-IR results of the AA biodegradable hydrogel and ZnO nanoflower on the AA biodegradable hydrogel are summarized in table 1. According to table 1, both the AA biodegradable hydrogel and ZnO nanoflower on the AA biodegradable hydrogel have the characteristic vibrational modes incident to AA (2942–293, 1695, 1452–1404, 1162–1155 and 795−788 cm^{-1}). The FT-IR result of the ZnO nanoflower clearly shows that the characteristic absorption peaks of Zn–O are nearer to 1541 cm^{-1}, these sharp characteristic peaks suggest the high-crystalline nature of ZnO nanoparticles. The peaks at 3835, 2152 and 2000 cm^{-1} also authenticate the presence of ZnO.

The thermal analysis of the ZnO nanoflower on the AA biodegradable hydrogel was performed to prove that the ZnO nanoflower has no influence on the AA biodegradable hydrogel negatively. The TGA thermogram of the sample showed a stability of the hydrogel substrate at 200°C (figure 3). Since the ZnO nanoflower produced on the AA biodegradable hydrogel was intended to be used in biological systems

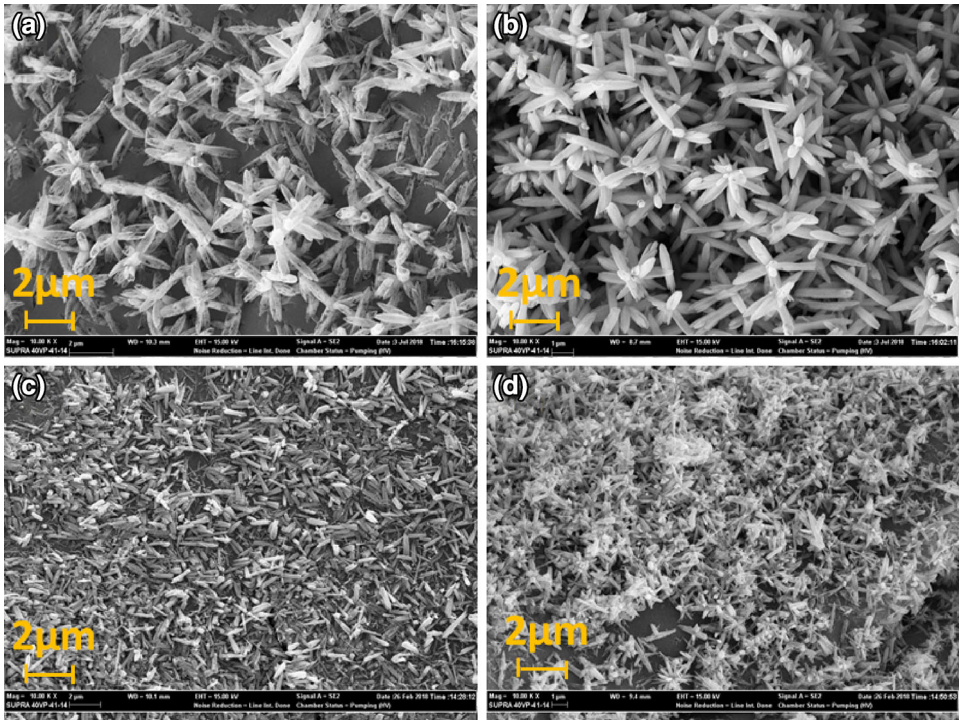

Figure 1. SEM images of ZnO nanoflower: (**a**) 15, (**b**) 30, (**c**) 45 and (**d**) 60 min.

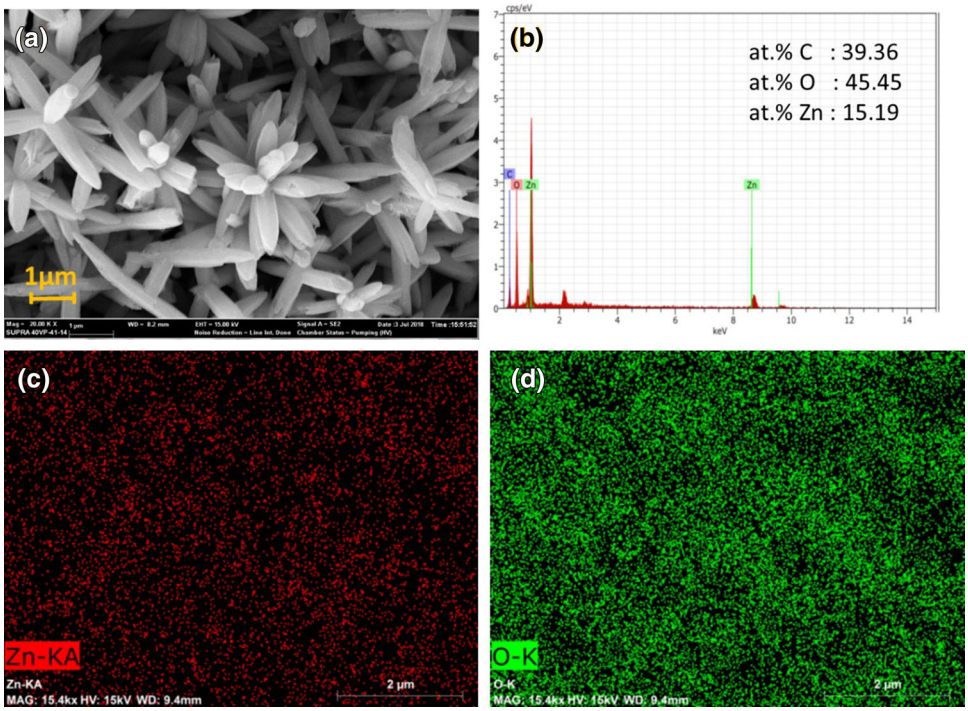

Figure 2. (**a**) SEM image, (**b**) elemental distribution and (**c**, **d**) elemental mapping of ZnO nanoflower at 30 min.

Table 1. FT-IR results of AA biodegradable hydrogel and ZnO nanoflower on AA biodegradable hydrogel.

Wavelength (cm^{-1})	Functional group	AA biodegradable hydrogel	ZnO nanoflower on AA biodegradable hydrogel
3835	Zn–O	—	Weak
2942–2935	C–H	Broad	Broad
2152	Zn–O	—	Weak
2000	Zn–O	—	Weak
1695	C=O	Sharp	Weak
1542	Zn–O	—	Sharp
1452–1404	C=O	Weak	Sharp
1162–1155	C–O–C	Sharp	Weak
795–788	C–H	Sharp	Weak
670–614	=C–H	Weak	Weak
518–503	C=O	Weak	Sharp

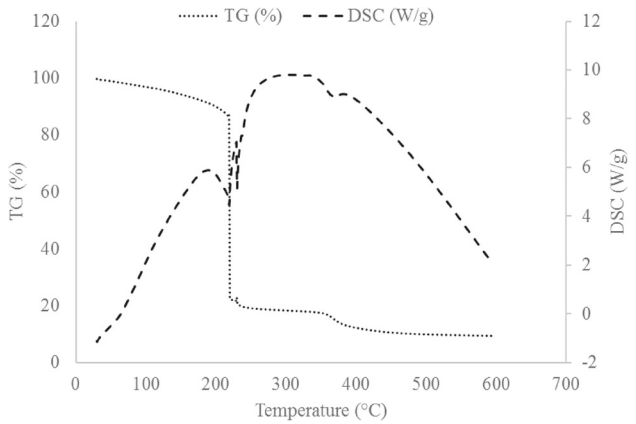

Figure 3. TG and dTG curves of ZnO nanoflower on AA biodegradable hydrogel.

as a biomaterial, and applications are normally carried out at a physiological temperature of 37°C; the produced sample is stable at room temperature, which normally varies between 27 and 38°C. The differential scanning calorimetry thermogram shows that the produced sample has characteristic peaks of AA at temperatures of 218 and 230°C. Due to the crystallization of ZnO an exothermic peak is observed at 390°C.

3.3 *Antibacterial activity of the AA biodegradable hydrogel and ZnO nanoflower on the AA biodegradable hydrogel*

Antibacterial activity tests were conducted on the AA biodegradable hydrogel and ZnO nanoflower on the AA biodegradable hydrogel. The results are shown in figures 4, 5 and table 2. The antibacterial tests indicated that the bacterial activity with *E. coli* on the AA biodegradable hydrogel and the ZnO nanoflower on the AA biodegradable hydrogel decreased by 57.03 and 97.14%, respectively. Antibacterial activity with the bacterium *S. aureus* on the AA biodegradable hydrogel

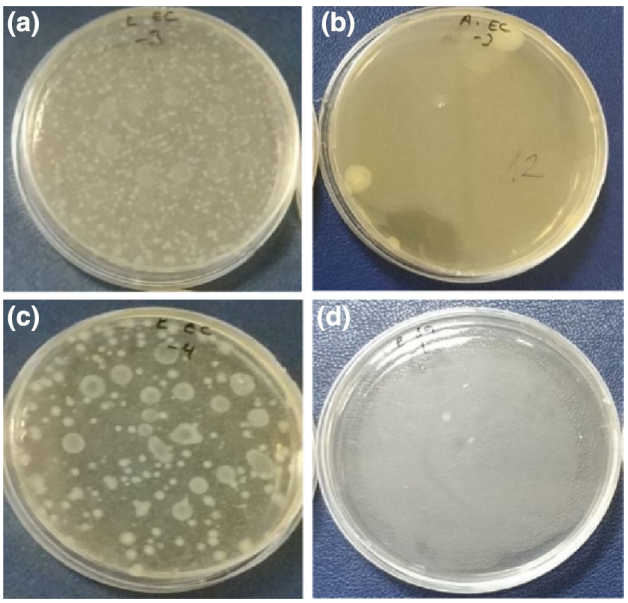

Figure 4. Antibacterial activity test images with the bacteria *E. coli*: AA biodegradable hydrogel count in the control sample (**a**) before and (**b**) after 24 h. ZnO nanoflower-deposited hydrogel count in the control sample (**c**) before and (**d**) after 24 h.

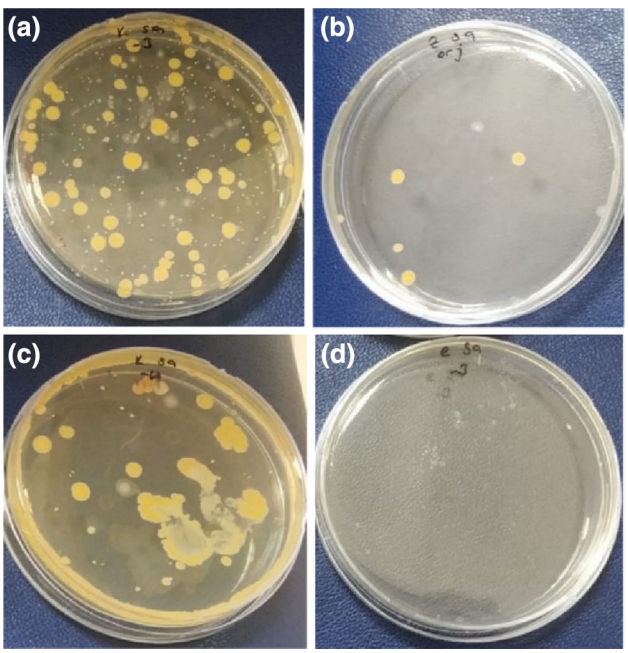

Figure 5. Antibacterial activity test images with the bacteria *S. aureus*: AA biodegradable hydrogel count in the control sample (**a**) before and (**b**) after 24 h. ZnO nanoflower-deposited hydrogel count in the control sample (**c**) before and (**d**) after 24 h.

decreased by 79.45% while the ZnO nanoflower on the AA biodegradable hydrogel decreased by 99.99%.

In previous studies, antibacterial activity of nano-ZnO particles on *E. coli* and *S. aureus* has been discussed by various

Table 2. Antibacterial activity test results of AA biodegradable hydrogel and ZnO nanoflower-deposited hydrogel.

Sample	Bacteria	Count in the control sample after 24 h	Count in sample after 24 h	Decrease (%)
AA biodegradable hydrogel	*E. coli*	490000	210553	57.03
ZnO nanoflower-deposited hydrogel	*E. coli*	490000	14000	97.14
AA biodegradable hydrogel	*S. aureus*	530000	108915	79.45
ZnO nanoflower-deposited hydrogel	*S. aureus*	530000	70	99.99

researchers. Zhang *et al* [21] have found that antibacterial behaviour of ZnO can be classified as chemical or physical interaction between ZnO and the microorganism cell envelope. The antibacterial mechanisms of microorganisms were specified depending on the ZnO morphology: (i) H_2O_2 generation, (ii) Zn^{2+} release from ZnO and (iii) the existence of oxygen vacancies onto the surface [22]. Thereby, the antibacterial properties of ZnO were established amenable to the generation of H_2O_2, while the maximum Zn^{2+} release as the bactericide mechanism was registered in the case of ZnO nano-flowers. According to physical interaction, Zn^{2+} penetrates through the cell wall and reacts with an inner constituent, then effects on viability of the cells. Chemical interaction between ZnO and the microorganism cell envelope causes the generation of H_2O_2.

In this study, it is also reported that ZnO in nano-size can penetrate through the cell wall easily, so the use of ZnO nanoparticles as antibacterial agents is more efficient than micro-ZnO particles.

4. Conclusion

In this study, an AA biodegradable hydrogel was synthesized by using an *in situ* free radical reaction. The produced hydrogels were used as substrates to deposit a ZnO nanoflower by a CBD technique for the first time reported in the literature. The deposition time plays a key role in obtaining flower-shaped nano-ZnO particles. Significant differences of morphological characteristics were observed by applying different deposition times of 15, 30, 45 and 60 min. The SEM images which represent the particles obtained at 30 min are flower-shaped with a narrow particle-size distribution. According to characterization studies, zinc and oxygen disperse on the hydrogel surface homogeneously. Both the AA biodegradable hydrogel and ZnO nanoflower on the AA biodegradable hydrogel have the characteristic vibrational modes incident to AA and the thermal analysis of the ZnO nanoflower on the AA biodegradable hydrogel proved that the ZnO nanoflower has no negative influence on the thermal stability of the hydrogel. Moreover, the deposited-ZnO nanoflower on the biodegradable hydrogel exhibited high activity against *E. coli* and *S. aureus*. As, zinc exists in the human body in a trace amount, ZnO-doped biodegradable nanocomposites can be used in the pharmaceutical, medical and food packaging industries.

Acknowledgements

This work was financially supported by the Scientific Research Project Commission of Bilecik Seyh Edebali University (Project Number is 2017-01.BŞEÜ.28-01). FT-IR and FESEM-EDX-Mapping measurements were performed in Bilecik Seyh Edebali University Central Research Laboratory. The antimicrobial activity tests were performed at Egemikal Environmental Health Laboratory. TG measurements were performed in Hacettepe University Advanced Technologies Application and Research Centre.

References

[1] Matei A, Cernica I, Cadar O, Roman C and Schiopu V 2008 *Int. J. Mater. Form.* **1** 767
[2] Priyanka G, Brian P, David W B, Wenjie H, William P J and Anne J A 2009 *J. Biol. Eng.* **3** 1
[3] Emami-Karvani Z and Chehrazi P 2011 *Afr. J. Microbiol. Res.* **5** 1368
[4] Rai M, Yadav A and Gade A 2009 *Biotechnol. Adv.* **27** 76
[5] Rizwan W, Young-Soon K, Amrita M, Soon-Il Y and Hyung-Shik S 2010 *J. Nanoscale Res. Lett.* **5** 1675
[6] Sawai J and Yoshikawa T 2003 *J. Microbiol. Methods* **54** 177
[7] Roselli M, Finamore A, Garaguso I, Britti M S and Mengheri E 2003 *J. Nutr.* **133** 4077
[8] Mohsen J and Zahra B 2008 *Afr. J. Biotechnol.* **7** 4926
[9] Laura K A, Delina Y L and Pedro J J A 2006 *J. Water Resour.* **40** 3527
[10] Sobha K, Surendranath K, Meena V, Jwala K T, Swetha N and Latha K S M 2010 *J. Biotechnol. Mol. Biol. Rev.* **5** 1
[11] Reddy K M, Kevin F, Jason B, Denise G W, Cory H and Alex P 2007 *J. Appl. Phys. Lett.* **90** 1
[12] Wahid F, Yin J J, Xue D D, Xue H, Lu Y S, Zhong C *et al* 2016 *Int. J. Biol. Macromol.* **88** 273
[13] Kalyani G, Anil V G, Bo-Jung C and Yong-Chien L 2006 *J. Green Chem.* **8** 1034
[14] Dobrucka R and Długaszewska J 2016 *Saudi J. Biol. Sci.* **23** 517
[15] Gunalan S, Sivaraj R and Rajendran V 2012 *Prog. Nat. Sci.: Mater. Int.* **22** 693

[16] Talebian N, Amininezhad S M and Doudi M 2013 *J. Photochem. Photobiol. B* **120** 66
[17] Karunakaran C, Rajeswari V and Gomathisankar P 2011 *Mater. Sci. Semicond. Process.* **14** 133
[18] Gokmen F O and Bayramgil N P 2017 *Eur. Chem. Bull.* **6** 514
[19] Temel S, Gokmen F O and Yaman E 2017 *Eur. Sci. J.* **13** 28
[20] Temel S, Gokmen F O and Yaman E 2017 *Int. J. Curr. Adv. Res.* **6** 4646
[21] Zhang L, Jiang Y, Ding Y, Daskalakis N, Jeuken L, Povey M *et al* 2010 *J. Nanopart. Res.* **12** 1625
[22] Dincă V, Mocanu A, Isopencu G, Busuioc C, Brajnicov S, Vlad A *et al* 2018 *Arab. J. Chem.* (in press)